

# Vibronic effects on resonant electron conduction through single molecule junctions

C. Benesch<sup>a,\*</sup>, M. Čížek<sup>b</sup>, M. Thoss<sup>a</sup>, W. Domcke<sup>a</sup>

<sup>a</sup> Department of Chemistry, Technical University of Munich, D-85747 Garching, Germany

<sup>b</sup> Charles University, Faculty of Mathematics and Physics, Institute of Theoretical Physics, Prague, Czech Republic

Received 14 June 2006; in final form 29 August 2006

Available online 9 September 2006

## Abstract

The influence of vibrational motion on electron conduction through single molecules bound to metal electrodes is investigated employing first-principles electronic-structure calculations and projection-operator Green's function methods. Considering molecular junctions where a central phenyl ring is coupled via (alkane)thiol-bridges to gold electrodes, it is shown that – depending on the distance between the electronic  $\pi$ -system and the metal – electronic–vibrational coupling may result in pronounced vibrational substructures in the transmittance, a significantly reduced current as well as a quenching of negative differential resistance effects.

© 2006 Elsevier B.V. All rights reserved.

## 1. Introduction

Recent advances in experimental studies of single molecule conduction [1–7] have stimulated great interest in the basic mechanisms which govern electron transport through nanoscale molecular junctions [8,9]. An interesting aspect that distinguishes molecular conductors from mesoscopic devices is the possible influence of the nuclear degrees of freedom of the molecular bridge on electron transport. The current-induced excitation of the vibrations of the molecule may result in heating of the molecular bridge and possibly breakage of the junction. Conformational changes of the geometry of the conducting molecule are possible mechanisms for switching behavior and negative differential resistance. Furthermore, the observation of vibrational structures in conduction measurements allows the unambiguous identification of the molecular character of the current.

Vibrational structures in molecular conductance were observed, for example, in electron transport experiments

on H<sub>2</sub> between platinum electrodes [3], as well as C<sub>60</sub> molecules between gold electrodes [2]. While in the latter two experiments the observed structures were attributed to the center of mass motion of the molecular bridge, other experiments on C<sub>60</sub>, C<sub>70</sub> [7], and copper phthalocyanin [6] on an aluminum oxide film showed structures which were related to the internal vibrational modes of the molecular bridge. Moreover, vibrational signatures of molecular bridges have also been observed in inelastic electron tunneling spectroscopy (IETS) [10,11].

This tremendous experimental progress has inspired great interest in the theoretical modelling and simulation of vibrationally-coupled electron transport in molecular junctions. In the low-voltage, off-resonant transport regime combinations of electronic-structure calculations and non-equilibrium Green's function theory (NEGF), employing the self-consistent Born approximation (SCBA), have been used to investigate vibrational signatures in IETS [12–14]. The majority of the studies in the resonant tunneling regime (for higher voltages) have been based on generic tight-binding models, using the NEGF–SCBA approach [15], or kinetic rate equations to calculate the current [16–21]. These model studies have demonstrated that the

\* Corresponding author.

E-mail address: [claudia.benesch@ch.tum.de](mailto:claudia.benesch@ch.tum.de) (C. Benesch).

vibrational motion of the molecular bridge may affect the current–voltage characteristics significantly.

Most of the studies of vibrationally-coupled electron transport reported so far invoke approximations which restrict their applicability either to small electronic–vibrational coupling, small molecule–lead coupling or separability of the vibrational modes. To circumvent this limitation, we recently proposed an approach [22–24], which is based on scattering theory and the projection-operator formalism of resonant electron-molecule scattering [25]. Within the single-electron description of electron conduction, this approach is valid for strong electronic–vibrational and molecule–lead coupling and thus allows the study of electron transport in the resonant regime. In the work reported here, the approach is combined with first-principles electronic-structure calculations to characterize the molecular junction. It is applied to investigate electron transport in two systems: *p*-benzene-dithiolate (BDT) and *p*-benzenedi(ethanethiolate) (BDET) covalently bound to gold electrodes (Fig. 1).

## 2. Theory

To study the influence of vibronic effects on single molecule conductance in BDT and BDET, we use an ab initio based model described by the Hamiltonian

$$H = \sum_{j \in M} |\phi_j\rangle E_j \langle \phi_j| + \sum_{k \in L,R} |\phi_k\rangle E_k \langle \phi_k| + V + H_n, \quad (1a)$$

$$V = \sum_{j \in M} \sum_{k \in L,R} (|\phi_j\rangle V_{jk} \langle \phi_k| + |\phi_k\rangle V_{kj} \langle \phi_j|). \quad (1b)$$

Here,  $|\phi_j\rangle$ ,  $j \in M$  and  $|\phi_k\rangle$ ,  $k \in L,R$  denote orthogonal electronic states (molecular orbitals) representing the molecular bridge and the left and right leads, respectively,  $E_j$  and  $E_k$  are the corresponding energies, and  $V$  characterizes the coupling strength between molecule

and leads. The nuclear degrees of freedom as well as the electron-nuclear coupling are described by  $H_n$ . Because the systems studied in this work do not exhibit large amplitude motion, we can employ the harmonic approximation and a low-order expansion of the molecular orbital energies around the equilibrium geometry of the neutral molecule. Thus, the nuclear part of the Hamiltonian reads

$$H_n = H_{n0} + H_{ne} = \sum_l \omega_l a_l^\dagger a_l + \sum_{j \in M,l} |\phi_j\rangle \kappa_l^{(j)} q_l \langle \phi_j|. \quad (2)$$

Here,  $a_l^\dagger$  and  $a_l$  are creation and annihilation operators for the  $l$ -th normal mode with dimensionless coordinate  $q_l$  and frequency  $\omega_l$ , and  $\kappa_l^{(j)}$  denotes the corresponding vibronic coupling constant in state  $|\phi_j\rangle$ .

For both systems investigated, the parameters of the Hamiltonian (1a) were determined employing electronic-structure calculations [26]. A detailed description of the strategy used will be given in a future publication. Briefly, the overall system was first separated into molecule and leads. The molecule and those parts of the leads which are close to the molecule (in the following referred to as the contacts) were treated explicitly in the quantum chemical calculations. A finite cluster of 30 gold atoms on each side of the molecule with a tip-like geometry was employed to model the contacts (cf. Fig. 1). A partial geometry optimization of the molecule and the first layer of the gold clusters was employed to determine a realistic molecule–lead binding geometry. Thereby, the sulfur atoms are bound covalently to two gold atoms, which is the preferred bond formation if no symmetry constraints are applied [4,27]. The effect of infinite leads can in principle be described employing the surface Green's function for the contacts [28]. In the present study, we have added constant selfenergies to the atomic orbital energies of the outer gold atoms of the contacts. After a Löwdin orthogonalization of the Kohn–Sham orbitals, the overall system was partitioned into molecule and contacts using projection-operator techniques [29]. A subsequent partial diagonalization of the Hamiltonian within the three subspaces (left contact, molecule, right contact) gives the electronic states  $|\phi_j\rangle$  and  $|\phi_k\rangle$ , representing the molecular bridge and the leads, the energies  $E_j$ ,  $E_k$  as well as the molecule–lead coupling matrix elements  $V_{jk}$ . The nuclear degrees of freedom of the molecular bridge were characterized based on a normal mode analysis of an extended molecule that includes seven gold atoms on each side of the molecule. The electronic–nuclear coupling constants  $\kappa_l^{(j)}$  were obtained from the gradients of the electronic energies  $E_j$  with respect to the normal coordinates  $q_l$ .

To investigate vibrationally inelastic electron transport through molecular junctions we shall consider the transmission probability of a single electron through the junction and the current–voltage characteristics. The inelastic transmission probability of a single electron from the left to the right lead as a function of initial and final electron energy is given by the expression

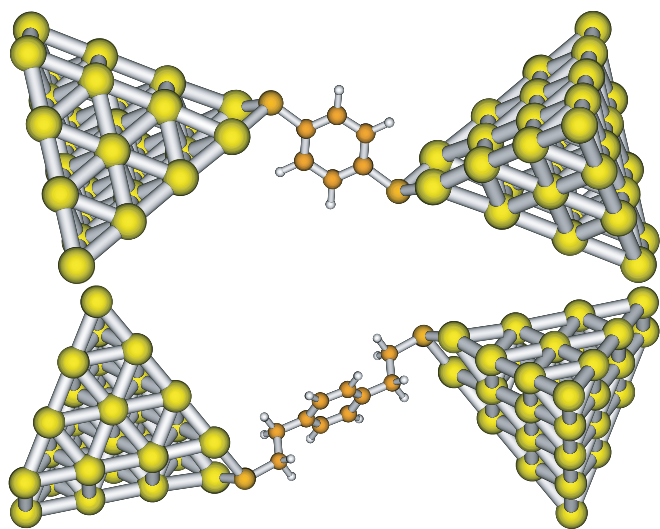


Fig. 1. The two molecular junctions investigated: BDT (top) and BDET (bottom) between clusters of 30 gold atoms.

$$\begin{aligned}
T_{R \leftarrow L}(E_i, E_f) &= 4\pi^2 \sum_{\mathbf{v}_i, \mathbf{v}_f} \sum_{k_i \in L} \sum_{k_f \in R} P_{\mathbf{v}_i} \delta(E_f + E_{\mathbf{v}_f} - E_i - E_{\mathbf{v}_i}) \\
&\quad \times \delta(E_i - E_{k_i}) \delta(E_f - E_{k_f}) \\
&\quad \times |\langle \mathbf{v}_f | \langle k_f | V G(E_i) V | k_i \rangle | \mathbf{v}_i \rangle|^2. \quad (3)
\end{aligned}$$

Here, the  $\delta$ -function accounts for energy conservation  $E_f + E_{\mathbf{v}_f} = E_i + E_{\mathbf{v}_i}$  with  $E_{\mathbf{v}_i}$  and  $E_{\mathbf{v}_f}$  being the energy of the initial and final vibrational states  $|\mathbf{v}_i\rangle$ ,  $|\mathbf{v}_f\rangle$ , respectively, and  $P_{\mathbf{v}_i} = \langle \mathbf{v}_i | \rho_0 | \mathbf{v}_i \rangle$  denotes the population probability of the initial vibrational state  $\rho_0 = e^{-H_{n0}/(k_B T)}/Z$ . In the systems considered in this work, the electron couples primarily to modes with relatively high frequencies. As a result, thermal effects are not expected to be of relevance and the initial vibrational state is assumed to be the ground state, i.e.  $\rho_0 = |\mathbf{0}\rangle\langle\mathbf{0}|$ . The total transmission probability,  $T_{R \leftarrow L}(E_i)$ , is obtained by integrating  $T_{R \leftarrow L}(E_i, E_f)$  over the final energy of the electron.

To calculate the transmission probability, the Green's function  $G(E) = (E^+ - H)^{-1}$  is projected onto the molecular space using the projection operators  $P = \sum_{j \in M} |\phi_j\rangle\langle\phi_j|$ ,  $Q_L = \sum_{k \in L} |\phi_k\rangle\langle\phi_k|$ , and  $Q_R = \sum_{k \in R} |\phi_k\rangle\langle\phi_k|$ , resulting in the expression

$$\begin{aligned}
T_{R \leftarrow L}(E_i, E_f) &= \sum_{\mathbf{v}_f} \text{tr} \{ \delta(E_f + E_{\mathbf{v}_f} - E_i - H_{n0}) \rho_0 \\
&\quad \times \Gamma_L(E_i) G_M^\dagger(E_i) | \mathbf{v}_f \rangle \langle \mathbf{v}_f | \Gamma_R(E_f) G_M(E_i) \}, \quad (4)
\end{aligned}$$

with the Green's function projected on the molecular bridge

$$G_M(E) = P G(E) P = (E^+ - PHP - \Sigma_L(E) - \Sigma_R(E))^{-1} \quad (5a)$$

$$\Sigma_L(E) = P V Q_L (E^+ - Q_L H Q_L)^{-1} Q_L V P = -\frac{i}{2} \Gamma_L(E) + A_L(E). \quad (5b)$$

Here,  $\Sigma_L(E)$  denotes the self energy due to coupling to the left lead and similar for the right lead.

It is noted that in contrast to purely electronic transport calculations as well as applications of the non-equilibrium Green's function formalism to vibronic transport [12,30], the Green's function  $G_M$  and the self energies  $\Sigma_L$ ,  $\Sigma_R$  are operators both with respect to the electronic and nuclear degrees of freedom. Thus, the Green's function has to be evaluated in the combined electronic–vibronic Hilbert space. To reduce the computational effort, in the calculations presented below, the four vibrational modes with the strongest vibronic coupling (as determined by the ratio of the electronic–vibronic coupling and the electronic coupling) were explicitly taken into account. Those are the C–C–C bending, the ring breathing (only for BDT), the C–C–H bending, and a C–C stretching mode, depicted in Figs. 2,3. The corresponding vibronic coupling constants in the most important molecular orbitals are given in Tables 1,2. Furthermore, the number of states  $|\phi_j\rangle$  on the molecular bridge, which were explicitly included in the calculation of the transmission, was reduced by including only those with energies in the vicinity of the Fermi energy (7 for BDT and 12 for BDET).

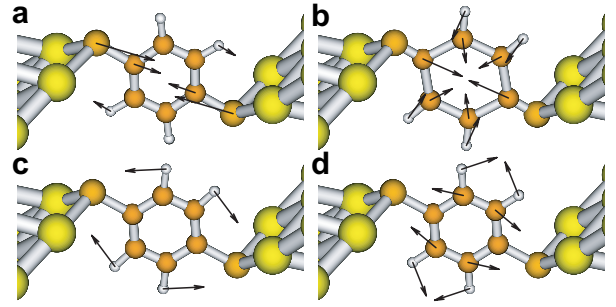


Fig. 2. Normal modes of BDT included in the calculation.

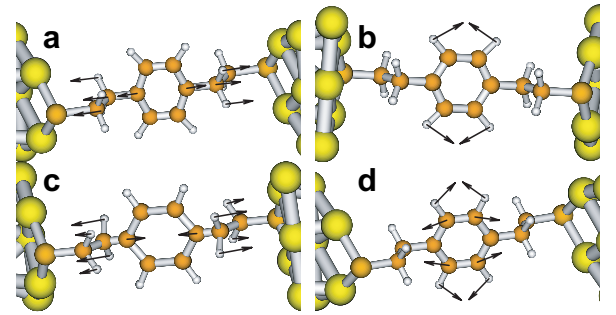


Fig. 3. Normal modes of BDET included in the calculation.

Based on the transmission probability (4), the current through the molecular junction is calculated using the generalized Landauer formula [31]

$$\begin{aligned}
I &= \frac{2e}{h} \int dE_i \int dE_f \{ T_{R \leftarrow L}(E_i, E_f) f_L(E_i) [1 - f_R(E_f)] \\
&\quad - T_{L \leftarrow R}(E_i, E_f) f_R(E_i) [1 - f_L(E_f)] \}, \quad (6)
\end{aligned}$$

Table 1

Frequencies of the four most important vibrational modes of BDT as well as gradients of these modes for the three orbitals (A, B, C) contributing to conduction

	$\omega$ (cm <sup>-1</sup> )	$\kappa_A$ (10 <sup>-1</sup> eV)	$\kappa_B$ (10 <sup>-1</sup> eV)	$\kappa_C$ (10 <sup>-1</sup> eV)
(a)	349.26	0.61	0.08	0.62
(b)	1092.02	0.72	0.80	0.33
(c)	1198.14	0.90	0.13	0.16
(d)	1627.28	1.52	0.93	0.36

Table 2

Frequencies of the four most important vibrational modes of BDET as well as gradients of these modes for the two orbitals (D, E) contributing to conduction

	$\omega$ (cm <sup>-1</sup> )	$\kappa_D$ (10 <sup>-1</sup> eV)	$\kappa_E$ (10 <sup>-1</sup> eV)
(a)	544.48	0.76	0.22
(b)	1197.11	0.51	0.69
(c)	1229.49	1.10	0.47
(d)	1671.56	1.36	1.62

where  $f_L(E)$ ,  $f_R(E)$  denote the Fermi distribution for the left and the right lead, respectively. While the formulas (3),(4) for the single-electron transmission probability involve no approximation, the expression (6) for the current is valid if many-electron processes are negligible. In particular, nonequilibrium effects in the leads and electron correlation due to electronic–vibrational coupling are not taken into account. Furthermore it is implicitly assumed, that the nuclear degrees of freedom of the molecular bridge relax to the vibrational equilibrium state after transmission of an electron.

In principle, the basis states  $|\phi_j\rangle$ ,  $|\phi_k\rangle$ , the electronic energies and the nuclear parameters depend on the bias voltage. For the studies in this work, we have used, for simplicity, parameters obtained from electronic-structure calculations at equilibrium and assumed that the bias voltage  $V$  enters the formulas only via the chemical potentials of the leads  $\mu_{L/R} = \epsilon_f \pm eV/2$ . Here  $\epsilon_f$  denotes the Fermi energy at equilibrium, which was approximated as the average of the energies of the HOMO and LUMO orbitals of the overall system. The energies of the lead states for finite voltage are thus given by  $E_k \pm eV/2$ . Since we do not invoke the wide-band approximation, the Green's function  $G_M$ , the self energies  $\Sigma_{L/R}$  as well as the width functions  $\Gamma_{L/R}$  also depend on the bias voltage.

### 3. Results and discussion

We first consider electron transport through BDT. Fig. 4a shows the total transmission probability for this system. In addition to the transmission based on a vibronic calculation, also the result of a purely electronic calculation (where all electronic–nuclear coupling constants  $\kappa_l^{(j)}$  were set to zero) is shown. The transmission probability exhibits several pronounced peaks. The first three peaks below  $\epsilon_f$  at energies  $-2.61$ ,  $-2.06$ , and  $-1.25$  eV, respectively, are caused by the three orbitals depicted in Fig. 4a. These orbitals are related to the  $e_{1g}$ -orbitals of benzene and p-orbitals at the sulfur atoms. While orbitals B and C have significant contributions from the bridging sulfur atoms, orbital A is completely localized on the phenyl ring. As a result, the molecule–lead coupling strength for the three orbitals is quite different: the width function,  $\Gamma_{jj}$ , at the respective peak energy varies from 0.01 eV (A), 0.07 eV (B) to 0.25 eV (C), respectively. Consequently, the structures in the transmission probability caused by orbitals B and C are rather broad, whereas orbital A results in a narrow peak. Besides structures at higher energies, the transmission probability also exhibits a broad peak close to  $\epsilon_f$ . Although this peak is influenced by orbitals B and C, it cannot be directly related to any of the orbitals of the molecular bridge and is therefore attributed to a metal-induced gap state [32,28]. As is known from scanning tunneling spectroscopy [33], the appearance of such states is expected for tip-like geometries of metal contacts as used in the present study.

The comparison of the vibronic transmission probability (solid line in Fig. 4a) with the results of the purely elec-

tronic calculation (dashed line) reveals that the electron–nuclear coupling in BDT has significant effects on the transmittance for narrow resonances. In particular, it results in a splitting of the narrow peak at  $-2.61$  eV into a number of smaller structures.

The effect of nuclear motion on the other peaks in the transmission probability is, on the other hand, rather small. This can be rationalized by considering the vibronic and electronic coupling constants in the corresponding states. The importance of vibronic effects caused by the nuclear mode  $q_l$  in state  $|\phi_j\rangle$  is determined by the ratio of the vibronic and electronic coupling constants,  $\kappa_l^{(j)}/\Gamma_{jj}$ . Although the electronic–vibrational coupling constants  $\kappa_l^{(j)}$  for some of the nuclear modes in states  $|\phi_B\rangle$  and  $|\phi_C\rangle$  are relatively large (cf. Table 1), the lifetime of the electron on the molecular bridge (approximately given by  $\hbar/\Gamma_{jj}$ ) is short – thus resulting in a small effective coupling  $\kappa_l^{(j)}/\Gamma_{jj}$ .

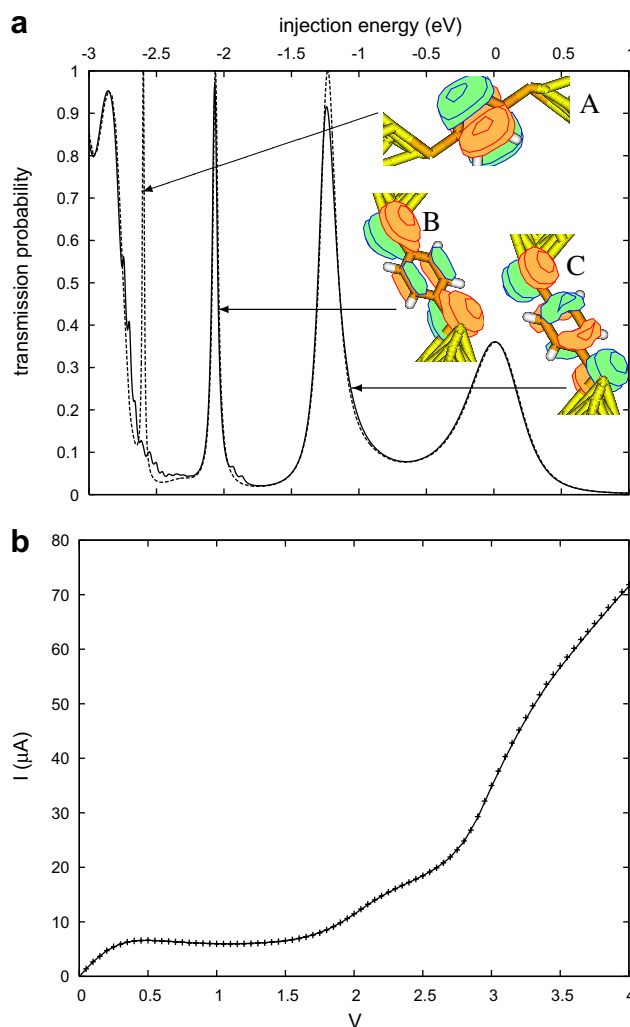


Fig. 4. (a): Electronic (dashed line) and vibronic (solid line) total transmission probability through a BDT molecular junction at zero voltage as a function of the initial energy of the electron (relative to the Fermi energy). The three localized molecular orbitals, denoted A, B, and C, dominate the transmittance at the indicated peaks. (b): Current–voltage characteristic of BDT. Shown are results of calculations with (solid line) and without (crosses) coupling to molecular vibrations.

The simulated current–voltage characteristic of BDT, depicted in Fig. 4b, exhibits a nonlinear behavior: A small increase of the current at small voltage caused by the metal-induced gap state at  $\epsilon_f$  is followed by a strong increase at larger voltage resulting from the contributions of orbitals B and C. Because orbitals B and C are strongly coupled to the metal leads and thus have a small effective vibronic coupling, the influence of nuclear motion on the current in BDT is almost negligible.

We next consider electron transport through BDET. In BDET, the  $(\text{CH}_2)_2$ -spacer groups reduce the electronic coupling between the conjugated  $\pi$ -system of the phenyl ring and the metal leads, which has a number of interesting consequences for the transport mechanism. The transmission probability for BDET is depicted in Fig. 5a. In contrast to the result for BDT, the transmission probability in the BDET system has only very little intensity at  $\epsilon_f$ . Thus, metal-induced gap states are of minor importance in this system. This is a consequence of the larger size of BDET and the smaller electronic coupling [28]. The resonance peaks at energies  $-2.24$  and  $-1.85$  eV, which are closest to  $\epsilon_f$  and thus determine the transport process, are caused by molecular orbitals D and E. While orbital D resembles an  $e_{1g}$ -orbital of benzene, orbital E has additional contributions at the spacer groups and the sulfur atoms. As a consequence, state D has small electronic coupling to the leads ( $\Gamma_{DD} = 2.1 \times 10^{-4}$  eV) resulting in a very narrow peak in the transmission probability, whereas the significant coupling of orbital E to the leads ( $\Gamma_{EE} = 8.9 \times 10^{-2}$  eV) results in a rather broad structure. Compared to the corresponding orbitals of the BDT system, the spacer group reduces the molecule–lead coupling by about an order of magnitude. As a result, the lifetime of the electron on the molecular bridge is significantly longer and thus effects due to nuclear motion become more important. The comparison between the results of vibronic (solid line in Fig. 5a) and purely electronic (dashed line) calculations demonstrates that the electronic–vibrational coupling in BDET alters the transmission probability significantly. In particular, the narrow peak (D) splits into many vibrational subpeaks, but also the broader peak (E) acquires substantial vibrational substructure. The vibrational structures can be assigned to the individual nuclear modes of BDET [29].

The current–voltage characteristics of BDET is shown in Fig. 5b. The result obtained from a purely electronic calculation (dashed line) shows an increase of the current at about 3.5 V caused by state E, which is followed by a pronounced decrease of the current at 4 V. The weakly coupled state D results only in a small step-like increase of the current at about 4.5 V. A detailed analysis [29] shows that the negative-differential resistance (NDR) effect at 4 V is caused by the voltage dependence of the self-energies  $\Sigma_L$ ,  $\Sigma_R$  and the corresponding width functions  $\Gamma$ . It should be emphasized that this NDR effect can only be described if the energy dependence of the self-energies is taken into account and will be missed within the often used wide-band

approximation. Including the coupling to the nuclear degrees of freedom changes the current–voltage characteristics substantially. In particular, the electronic–vibrational coupling results in a quenching of the NDR effect, a significantly smaller current for voltages in the range 3.5–4.25 V, and noticeable vibrational structures in the current. The smaller current and the vibrational substructures are a result of the splitting of each electronic resonance into several vibronic resonances (cf. Fig. 5a), which contribute with different weights (determined by the respective Franck–Condon factors) to the transmission. In contrast to the purely electronic case, the current thus increases in several steps. This effect is well known from previous model studies

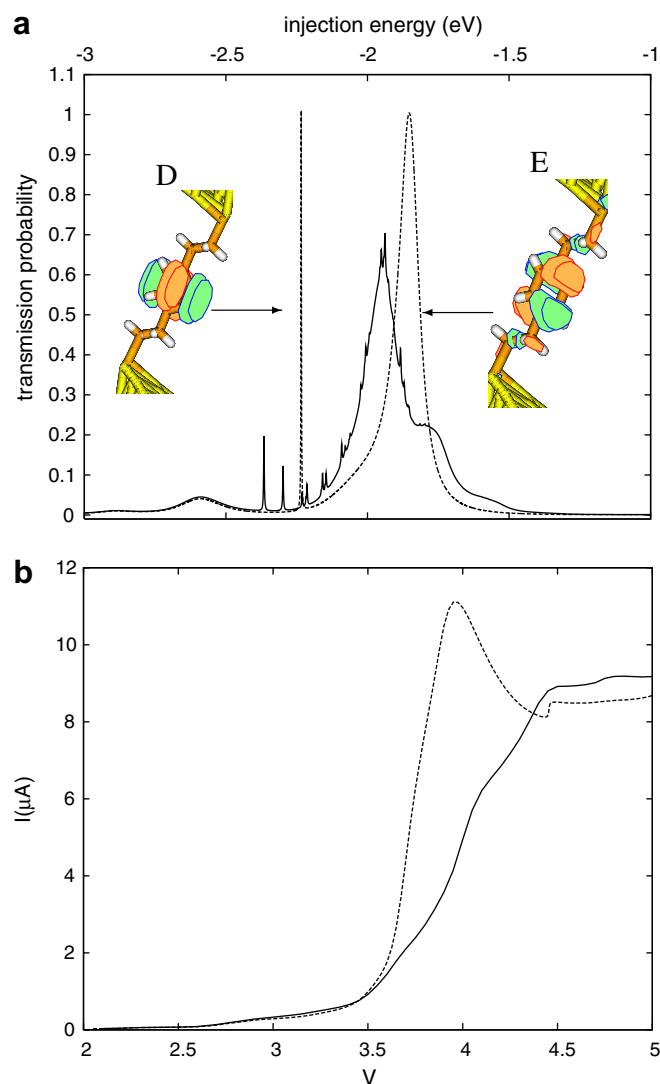


Fig. 5. (a): Electronic (dashed line) and vibronic (solid line) total transmission probability through a BDET molecular junction at zero voltage as a function of the initial energy of the electron (relative to the Fermi energy). The two orbitals, denoted D and E, dominate the transmittance at the indicated peaks. (b): Current–voltage characteristic of BDET. Shown are results of calculations with (solid line) and without (dashed line) coupling to molecular vibrations.

[22,20]. The quenching of the NDR effect, on the other hand, is caused by a subtle interplay between the voltage dependence of the self energies and the Pauli-blocking factors in the formula for the current and will be analysed in more detail elsewhere [29].

Finally, it is noted that the overall current through BDET is about an order of magnitude smaller than in BDT. This is a result of the  $(\text{CH}_2)_2$ -spacer groups, which reduce the effective coupling between phenyl-ring and gold leads. A similar reduction of the current was also found in experimental studies of electron transport through benzenedimethanethiol [5].

#### 4. Conclusion

The theoretical studies reported in this work demonstrate that nuclear motion can have a significant effect on electron conduction through single molecule junctions. The importance of vibronic effects thereby depends crucially on the relative ratio between electronic–vibrational coupling and molecule–lead interaction. While the former is determined by the character of the electronic states of the molecular bridge, the latter can be varied systematically, e.g., by introducing spacer groups between molecule and leads. To study these effects, we have considered in this work two systems, BDT and BDET, covalently bound to gold electrodes. In BDT, an example for a molecular junction with strong coupling to the leads, electronic–vibrational coupling results in vibrational sidebands in the transmission probability, but the effect is rather small and the influence on the current is almost negligible. In BDET, on the other hand, a system where spacer groups reduce the molecule–lead coupling by about an order of magnitude, vibronic effects change the current–voltage characteristics substantially. In particular, it was found to result in quenching of NDR-effects, a significantly reduced current over a range of voltages, as well as vibronic structures in the current–voltage characteristics.

#### Acknowledgement

This work has been supported by the Deutsche Forschungsgemeinschaft.

#### References

- [1] M. Reed, C. Zhou, C. Muller, T. Burgin, J. Tour, *Science* 278 (1997) 252.
- [2] H. Park, J. Park, A. Lim, E. Anderson, A. Alivisatos, P. McEuen, *Nature (London)* 407 (2000) 57.
- [3] R. Smit, Y. Noat, C. Untiedt, N. Lang, M. van Hemert, J. van Ruitenbeek, *Nature (London)* 419 (2002) 906.
- [4] H.B. Weber, J. Reichert, F. Weigend, R. Ochs, D. Beckmann, M. Mayor, R. Ahlrichs, H.v. Löhneysen, *Chem. Phys.* 281 (2002) 113.
- [5] X. Xiao, B. Xu, N. Tao, *Nano Lett.* 4 (2004) 267.
- [6] X. Qiu, G. Nazin, W. Ho, *Phys. Rev. Lett.* 92 (2004) 206102.
- [7] N. Liu, N. Pradhan, W. Ho, *J. Chem. Phys.* 120 (2004) 11371.
- [8] P. Hänggi, M. Ratner, S. Yaliraki, (Eds.), *Chem. Phys. special issue on: Processes in molecular wires*, 281.
- [9] A. Nitzan, M. Ratner, *Science* 300 (2003) 1384.
- [10] B. Stipe, M. Rezai, W. Ho, *Science* 280 (1998) 1732.
- [11] J. Kushmerick, J. Lazorcik, C. Patterson, R. Shashidhar, D.S. Seferos, G.C. Bazan, *Nano Lett.* 4 (2004) 639.
- [12] A. Pecchia, A.D. Carlo, *Nano Lett.* 4 (2004) 2109.
- [13] Y. Chen, M. Zwolak, M.D. Ventra, *Nano Lett.* (5) (2005) 813.
- [14] M. Paulsson, T. Frederiksen, M. Brandbyge, *Phys. Rev. B* 72 (2005) 201101.
- [15] M. Galperin, M. Ratner, A. Nitzan, *Phys. Rev. B* 73 (2006) 045314.
- [16] E. Emberly, G. Kirczenow, *Phys. Rev. B* 61 (2000) 5740.
- [17] D. Boese, H. Schoeller, *Europhys. Lett.* 54 (2001) 668.
- [18] V. May, *Phys. Rev. B* 66 (2002) 245411.
- [19] J. Lehmann, S. Kohler, V. May, P. Hänggi, *J. Chem. Phys.* 121 (2004) 2278.
- [20] J. Koch, F. von Oppen, *Phys. Rev. Lett.* 94 (2005) 206804.
- [21] K. Nowack, M. Wegewijs, *New J. Phys.* 7 (2005) 239.
- [22] M. Cizek, M. Thoss, W. Domcke, *Phys. Rev. B* 70 (2004) 125406.
- [23] M. Cizek, M. Thoss, W. Domcke, *Czech. J. Phys.* 55 (2005) 189.
- [24] A closely related approach has been proposed by Ness et al. [34].
- [25] W. Domcke, *Phys. Rep.* 208 (1991) 97.
- [26] All quantum chemical calculations were performed with the TURBOMOLE package (V5-7) [35] using density functional theory (DFT) with the B3-LYP functional and the SV(P) basis set including ECP-60-MWB on the gold atoms.
- [27] H. Basch, M.A. Ratner, *J. Chem. Phys.* 119 (2003) 11926.
- [28] Y. Xue, M. Ratner, *Phys. Rev. B* 68 (2001) 115406.
- [29] C. Benesch, M. Cizek, W. Domcke, M. Thoss, in preparation.
- [30] D.A. Ryndyk, M. Hartung, G. Cuniberti, *Phys. Rev. B* 73 (2006) 045420.
- [31] A. Nitzan, *Annu. Rev. Phys. Chem.* 52 (2001) 681.
- [32] R. Guitierrez, G. Fagas, K. Richter, F. Grossmann, R. Schmidt, *Europhys. Lett.* 62 (2003) 90.
- [33] A.V. de Parga, O. Hernan, R. Miranda, A.L. Yeyati, N. Mingo, A. Martin-Rodero, F. Flores, *Phys. Rev. Lett.* 80 (1998) 357.
- [34] H. Ness, S. Shevlin, A. Fisher, *Phys. Rev. B* 63 (2001) 125422.
- [35] R. Ahlrichs, M. Bär, M. Häser, H. Horn, C. Kölmel, *Chem. Phys. Lett.* 162 (1989) 165.